A Theoretical Study of Hydroxycarbene as a Model for the Homolysis of Oxy- and Dioxycarbenes

Darren L. Reid, Jesús Hernández-Trujillo,† and John Warkentin*

Department of Chemistry, McMaster University, Hamilton, Ontario, Canada L8S 4M1

Received: November 30, 1999

Recent work has shown that dioxycarbenes can readily undergo homolytic fragmentations to radicals in solution. Previous workers have found some theoretical evidence for a transition state in the homolysis of dihydroxycarbene to HOCO and H radicals using the CISD method, but they were not able to conclude whether such a barrier was real or an artifact of the approximation. In this work the homolysis of hydroxycarbene is examined at the CAS and MRCI levels of theory using the cc-pVDZ basis set. The atomic and molecular properties are examined using the theory of atoms in molecules. At the highest level of theory, a transition state is found for the fragmentation of *trans*- but not of *cis*-hydroxycarbene. This transition state is rationalized in terms of the electronic states involved in the avoided crossing and by examining the evolution of several atomic and molecular properties during the homolysis. It is concluded that its origin can be traced to a mismatch of the electronic structures of these states in the region of the avoided crossing, best expressed by the dipole moments.

1. Introduction

Facile unimolecular reactions of carbenes in solution include [1,2]-migrations (particularly of H), insertions into a more remote σ-bond in one of the carbene substituents, and addition to a similarly situated π-bond.[1−3] Oxy- and dioxycarbenes, reactive intermediates of considerable practical and theoretical importance, are also believed to undergo fragmentation to radicals either photochemically or thermally. Homolysis of cyclic oxycarbenes, generated by the photolysis of cycloalkanones, to acyl alkyl biradicals has been suggested[4,5] and established.[6] Ring opening of cyclic oxy-[7−10] and dioxycarbenes[11] has been proposed in a number of cases where the carbenes were generated by the pyrolysis of tosylhydrazones at temperatures ranging from 190 to 210 °C. It has also been proposed that acyclic oxy- and dioxycarbenes decompose to radical pairs when generated thermally by the tosylhydrazone route at 158 and 175 °C in solution.[12,13] Lemal et al. suggested that dimethoxycarbene, generated by the vapor-phase pyrolysis of norbornadienone ketals at 200 °C, fragments to methyl and methoxycarbonyl radicals.[14,15] Vibrationally excited dimethoxycarbene[16] and 2,2,2-trifluoroethoxymethoxycarbene,[17] generated in neutralization−reionization mass spectrometry experiments from oxadiazoline precursors, are also believed to fragment to radicals. Hoffmann et al. used labeling studies to show that the esters derived from the gas-phase pyrolysis of 7-methoxy-7-allyloxy-bicyclo[2.2.1]heptadiene and 7,7-diallyloxy-bicyclo-[2.2.1]heptadiene at 250 °C come from a radical route, likely through the allyloxy-substituted carbenes.[18] Recent carbene and radical trapping studies by Venneri and Warkentin provided strong evidence for the thermal fragmentation of allyloxymethoxycarbenes to radicals in solution at 110 °C to give the products of apparent [1,2] and [2,3]-sigmatropic rearrangements (1).[19]

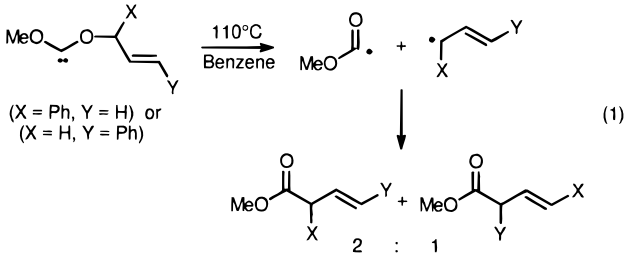

These results suggest that homolysis to radical pairs might be a general and facile reaction of oxy- and dioxycarbenes.

Surprisingly, there has been very little theoretical consideration given to the mechanisms for homolysis of oxy- and dioxycarbenes. Some computational work on the photochemical rearrangement of cyclic carbonyl compounds to oxycarbenes indirectly explored a triplet mechanism for the homolysis of oxycarbenes.[20,21] The triplet (T_1) state ($n-\pi^*$) of the oxycarbene would be reached either photochemically or thermally, by intersystem crossing, followed by β-scission to give the biradical. Borden et al. studied the homolysis of the w-conformer of dihydroxycarbene from its singlet ground state (S_0) and found the H and COOH radicals to be 48 kcal mol^{-1} (CISD/STO-3G) above the carbene (43 kcal mol^{-1} at the CISD/DZP level).[22] These authors also found an additional barrier of ∼3 kcal mol^{-1} for fragmentation to the radicals, but they were not able to conclude from their results whether such a barrier was real. They suggested that the fragmentation should be similar to the homolysis of formaldehyde to the same radicals, which was previously reported to occur without a transition state.[23] The same view was expressed by Saito et al. when they suggested homolysis as a pathway for dihydroxycarbene.[24] They pointed out that for simple scission reactions the threshold energies can be nearly equal to the heats of reaction. These disparate results suggested the importance of further study, which could lead to a better understanding of the mechanism of homolysis of oxy- and dioxycarbenes from the singlet ground state.

† Permanent address: Departamento de Física y Química Teórica, Facultad de Química, Universidad Nacional Autónoma de México, México, D.F. 04510, Mexico.

10.1021/jp9941965 CCC: $19.00
Published on Web 03/28/2000

SCHEME 1

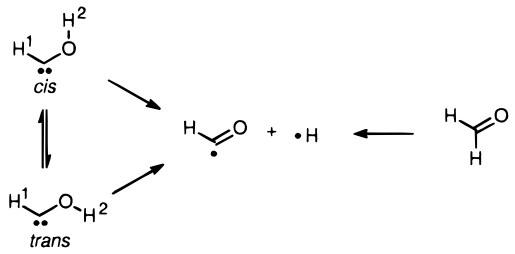

In this paper the dissociation of hydroxycarbene (HCOH) is used as a model for the more complex oxy- and dioxycarbenes, which do appear to undergo homolysis from a singlet ground state. Scheme 1 shows the dissociation of the stable cis and trans isomers. As the homolysis of formaldehyde (H_2CO) yields the same radicals, it is included in this work as a test for the methods used. The systems were modeled using complete active space and multireference configuration interaction methods. The potential energy surfaces are analyzed, and the theory of atoms in molecules (AIM)[25] is used in the discussion of the electronic structure of the molecules.

2. Analysis of the Atomic and Molecular Properties

The theory of atoms in molecules provides a rigorous definition of an atom in a molecule and provides the means to obtain its properties.[25] Within this theory, an atom in a molecule is defined as an open subset in real space that generally contains an atomic nucleus and whose boundary is a zero-flux surface of electron density gradient. Such a boundary can be considered as the union of interatomic surfaces that define the interactions between pairs of atoms in the molecule. For each interatomic surface there is a pair of gradient paths that go to each of the associated atomic nuclei. These gradient paths start from a common point on the interatomic surface, which corresponds to a critical point of the electron density and is called a bond critical point. It is over the volume defined by the atomic basin that the observables are integrated to yield the corresponding atomic properties. Examples of such atomic properties are the charge, the first moment of the electron density, and the energy.

The analysis of the dipole moment ($\boldsymbol{\mu}$) of the molecule, in terms of the atomic charges and atomic first moments, has proved to be useful in understanding the polarization of a given charge distribution.[25,26] If $\{\mathbf{R}_\alpha\}$ denotes the set of nuclear coordinates referred to an arbitrary origin and $\{\mathbf{M}_\alpha\}$ the atomic moments of a given molecule, the dipole moment can be written as $\boldsymbol{\mu} = \sum_\alpha q_\alpha \mathbf{R}_\alpha + \sum_\alpha \mathbf{M}_\alpha = \boldsymbol{\mu}_{ct} + \boldsymbol{\mu}_p$. In this expression $\boldsymbol{\mu}_{ct}$ and $\boldsymbol{\mu}_p$ are called the charge-transfer and polarization contributions, respectively. For a neutral molecule, $\boldsymbol{\mu}$ and its contributors $\boldsymbol{\mu}_{ct}$ and $\boldsymbol{\mu}_p$ are origin independent. This allows the partitioning of the dipole moment into contributions readily interpretable in physical terms. That is, $\boldsymbol{\mu}_{ct}$ results from the transfer of charge among the atoms in the molecule and represents the contribution to the dipole moment of a set of spherical charge densities. On the other hand, $\boldsymbol{\mu}_p$ accounts for the nonsphericity of the atoms in the molecule, as the atomic moments indicate the direction of polarization of the electron density in each of the atoms.

The Laplacian of the electron density ($\nabla^2\rho(\mathbf{r})$) is also an important property, for it contains information about the electron structure that is not directly available from the electron density.[25,27] For example, it has been shown that $\nabla^2\rho(\mathbf{r})$ displays the shell structure of free atoms as well as of atoms in a molecule and that negative values of $\nabla^2\rho(\mathbf{r})$ refer to points in space where the electron density is locally concentrated or depleted. It has been suggested that the critical points defined by the minima in the Laplacian of the electron density can be used to identify, for example, a lone pair in a molecule and also provide a physical basis for the VSEPR model.[28]

3. Computational Methods

Calculations of the wave functions and optimizations for HCOH and its isomers were carried out using the general atomic and molecular electronic structure system of programs (GAMESS, version 6 MAY 1998).[29] Dunning's correlation-consistent, polarized-valence, double-zeta (cc-pVDZ) basis set was found to be appropriate for the study.[30] Geometries were optimized using the quasi-Newton−Raphson search with the quadratic approximation algorithm at the complete active space self-consistent-field (CASSCF) level of theory using several choices of active space. It was determined that in order to describe the dissociation processes correctly, the active space should include at least eight electrons and eight active in-plane orbitals to give an 8,8 active space (CAS(8,8)). This active space was augmented with the two lowest energy out-of-plane π orbitals to give a 10,10 active space (CAS(10,10)), which was also utilized in the study. The modeling of the homolysis of *cis*- and *trans*-HCOH at the CAS(10,10) level, using only the O−H bond length as a constraint, indicated that the dissociation proceeded in plane. Frequency calculations at the CAS(10,10) level indicated only one imaginary frequency for the transition states. As a consequence, both active spaces were employed to study the dissociation from the ground state (S_0), using the symmetry plane and the dissociating bond distance as constraints for the optimizations. The first singlet excited state (S_1) was calculated for the vertical excitation at the state-averaged CASSCF level of theory with averaging of the S_0 and S_1 states using the CAS(10,10) ground-state (S_1) geometries. In these calculations, equal weights were given to each of the states.

Single-point multireference configuration interaction (MRCI) calculations were performed using the 8,8 active space (MRCI(8,8)) at the corresponding CASSCF optimized geometries. These MRCI(8,8) calculations included all single and double excitations from the CASSCF active space and provided the wave functions for the analysis of the electron density of the HCOH isomers. Calculations of the atomic properties defined by the theory of atoms in molecules were performed using the AIMPAC system of programs.[31] The formyl radical was also examined. The ground-state wave function of this doublet was calculated at the SD-CI/cc-pVDZ level of theory, including all possible excitations from core and valence orbitals in the CI expansion, using the Gaussian94, Revision E.2, system of programs.[32] This wave function was used to integrate the spin densities over the atomic basins in the radical.

4. Results and Discussion

4.1. Potential Energy Surfaces. Figure 1 shows the potential energy curves for the dissociation of *cis*- and *trans*-HCOH at the CAS(8,8) and the CAS(10,10) levels. To evaluate the performance of these levels of theory, the analogous H_2CO dissociation is also included. In addition, Table 1 displays the energies for the equilibrium geometries, the approximate barrier heights, and the dissociation energies. A number of important points should be noted from these results. As expected, all three isomers dissociate to the same limit. At the equilibrium geometry the trans isomer is the lowest energy conformer of HCOH, in agreement with conclusions of previous workers.[20,23,33−38] For both CAS levels of theory, the calculated dissociation energies of formaldehyde are in good agreement with the experimental

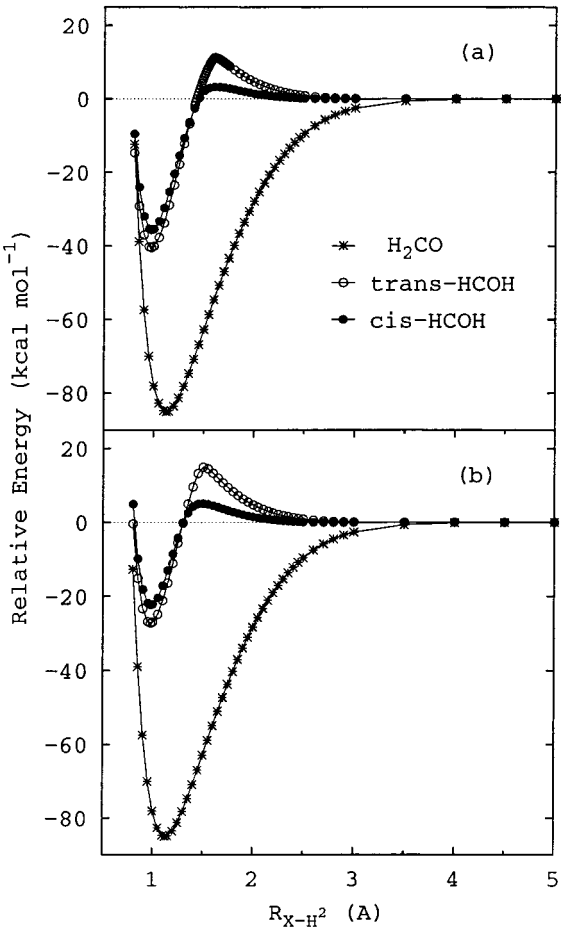

Figure 1. Potential energy curves for the homolysis of *cis*-HCOH, *trans*-HCOH, and H_2CO: (a) at the CAS(8,8) level of theory and (b) at the CAS(10,10) level of theory.

TABLE 1: Energies for Important Points on the Dissociation Curves for Each Isomer (in kcal mol^{-1}) at All Levels[a]

level	isomer	eq. geom.	TS barrier	R_{X-H} = 7.0 Å
CAS(10,10)/cc-pVDZ	*cis*-HCOH	−22.37	5.09	(−113.894618)
	trans-HCOH	−27.26	14.92	0.00
	H_2CO	−84.97	no TS	0.00
CAS(8,8)/cc-pVDZ	*cis*-HCOH	−35.74	3.24	(−113.822002)
	trans-HCOH	−40.52	11.25	0.00
	H_2CO	−85.04	no TS	0.00
MRCI(8,8)/cc-pVDZ//	*cis*-HCOH	−44.79	no TS	(−113.900490)
CAS(8,8)/cc-pVDZ	*trans*-HCOH	−49.37	6.03	0.00
	H_2CO	−85.91	no TS	0.00

[a] All energies are given relative to the radicals for dissociation of *cis*-HCOH at 7.0 Å, whose total energy (hartrees) is given in parentheses for each active space.

value of 87.1 kcal mol^{-1}, calculated from the heats of formation of the radicals and formaldehyde.[39] Previous calculations using a DZ basis set with polarization functions and SD-CI gave a dissociation energy of 88.5 kcal mol^{-1}, which was lowered to 80.2 kcal mol^{-1} after an experimental zero-point vibrational energy (ZPVE) correction was added.[23] In a more recent study, where the radicals were calculated as doublets at the MP4-(SDTQ)/6-311G**//MP2/6-31G* level, with a ZVPE correction of 8.7 kcal mol^{-1} and annihilation of spin contamination, it was found that the radicals were 80.1 kcal mol^{-1} above formaldehyde.[34] Note that the dissociation energies in Table 1 were not corrected for the ZPVE. The CAS(10,10) results are in better agreement with the energy difference of 54.2 ± 2 kcal mol^{-1}

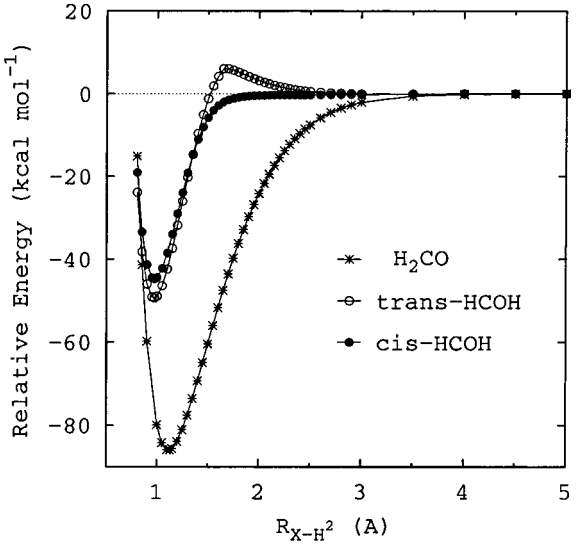

Figure 2. Potential energy curves for the homolysis of *cis*-HCOH, *trans*-HCOH, and H_2CO at the MRCI(8,8) level of theory.

found between HCOH and formaldehyde by cyclotron double-resonance spectroscopy.[40] The CAS(10,10) value for the HCOH and formaldehyde energy difference is also in good agreement with previous theoretical work.[20,23,33,34,36−38,41] Consistent with other theoretical calculations,[21] H_2CO does not have a transition state (TS) in its homolysis at either level of theory. However, for both active spaces the *cis*- and *trans*-HCOH homolysis curves do have maxima, with the one for *trans*-HCOH being the most pronounced.

The main objectives of this work were to determine if there is a transition state for the homolysis of oxy- and dioxycarbenes, and to understand the underlying physical nature of this process. Since both active spaces show similar dissociation curves, the 8,8 active space was selected to include dynamic electron correlation by means of MRCI calculations, which would not be possible with the larger 10,10 active space due to computational limitations. Figure 2 shows the MRCI(8,8) potential energy curves for *cis*-HCOH, *trans*-HCOH, and H_2CO as a function of the reaction coordinate. The energy of the carbenes relative to both formaldehyde and the radicals is less than that from the CAS results. Most remarkably, the maximum in the *trans*-HCOH potential energy surface remains while it disappears for the *cis*-HCOH surface. Borden et al. have reported that the dissociation of singlet carbenes might involve the existence of a transition state.[22] However, their observation resulted from use of single-determinant wave functions, and they were unable to exclude the possibility that such behavior was due to an inadequacy of the method of calculation used.

To investigate further the nature of the transition state observed for *trans*-HCOH, state-averaged CAS(10,10) calculations involving the S_0 state and the vertical S_1 state were carried out for the dissociation of both *cis*- and *trans*-HCOH. Note that this work was not an attempt to study the first excited singlet state of hydroxycarbene, whose geometry is thought to be gauche.[36] The analysis of the vertical S_1 state is included only to analyze its effect on the ground state in the vicinity of the avoided crossing of states of the same symmetry. Figure 3 shows the avoided crossing in the region of the transition state. On the carbene side of the potential energy curve the excited state involves an important contribution of an excitation from the lone pair of the carbon atom to the σ^* orbital of the breaking O−H bond ($n \rightarrow \sigma^*$) to give an $n^1\sigma^1$ configuration. Beyond the avoided crossing of states, this configuration becomes the main

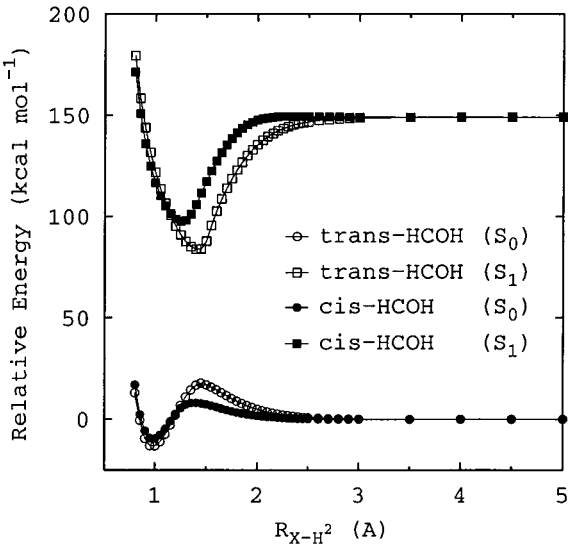

Figure 3. S_0 and S_1 potential energy surfaces of *cis*- and *trans*-HCOH at the state-averaged CAS(10,10) level.

contribution corresponding to the ground state of the radicals. In effect, this suggests that the hydrogen atom leaves with an electron from the carbene lone pair (n^2) and not from the O−H σ bond, a point that will become clearer from the analysis of the electronic properties in the following sections. This result could be contrasted with some previous studies which have predicted that S_1 for hydroxycarbene, methoxymethylcarbene, and dimethoxycarbene would comprise an important contribution of the $n^1\pi^1$ configuration resulting from an excitation from the carbon lone pair to π^*.[36,42,43] This could be a consequence of the use of single-reference-correlated wave functions in those studies. As was the case for the pure-state CAS calculations, there is a maximum in the potential energy curves of both conformers, but it is expected that at the MRCI level the one for the cis conformer will disappear. Due to computational limitations, the MRCI(10,10) state-averaged calculations could not be performed. Although both conformers have maxima, some qualitative conclusions can be drawn. As can be seen from Figure 3, the avoided crossing of states should occur first for the dissociation of the cis conformer. This is in part due to the steeper increase in the energy of the ground state for this conformer in comparison to *trans*-HCOH. As a result, the trans conformer maintains its carbene-like configuration (n^2) farther along the reaction coordinate.

4.2. Electronic Properties. The changes in the electronic structure of HCOH can be analyzed in terms of the properties of the atoms defined by the theory of atoms in molecules, as well as the local properties of the electron density ($\rho(\mathbf{r})$). The following analysis for each HCOH conformer was performed using MRCI(8,8) wave functions for a number of R_{O-H} values. The atomic charges are displayed in Figure 4, including those for the homolysis of the C−H bond of formaldehyde for comparison. In the case of the leaving hydrogen atom the final charge corresponds to the free atom. The evolution of the atomic charges during the homolysis of the HCOH conformers indicates that early in the dissociation the leaving hydrogen atom withdraws electron density from oxygen. However, it is carbon that loses electron density to hydrogen and oxygen in the region of the avoided crossing of states due to the transition from the n^2 to the $n^1\sigma^1$ configuration. As a result, the net change in the atomic charge of oxygen is small as the carbene is transformed to radicals. A simple analysis of the formyl radical in terms of Lewis structures indicates that the spin density should be highly localized on the carbon atom. At the SD-CI/cc-pVDZ level of theory, the populations are 0.5545, 0.2731, and 0.1724 α-electron for C, O, and H, respectively. These values are obtained by intergration of the spin density over the atomic basins. Previous workers have shown that the spin density is spread over the entire molecule,[44,45] but the integrated values above also indicate that this is a carbon-centered radical. These spin densities emphasize the point that, at the avoided crossing of states, the carbon lone pair gives up electron density to become the radical center. This result is also in agreement with the potential energy curves in Figures 1 and 2, which show that the reverse reaction, the approach of the H atom to the HCO radical, would give formaldehyde as the preferred product.

It is also useful to compare the relative values of the charges of the atoms in the conformers. In the trans conformer the system retains more carbene character as it approaches the avoided crossing of states, and there is a buildup of the atomic charge on oxygen that occurs farther along the reaction coordinate relative to *cis*-HCOH. This indicates that the carbon atom is less able to donate electron density to oxygen in the trans system when the carbene begins to dissociate. This behavior should be contrasted to the observed trends for the atomic charges in formaldehyde (Figure 4b), where there is no such dramatic change in the values during dissociation. It is necessary to stress the relationship between this behavior of the atomic charges of the three isomers and that of the corresponding potential energy surfaces. Formaldehyde does not exhibit a transition state, and its atomic charges display a monotonic behavior. Moreover, due to the persistence of its n^2 electronic state, *trans*-HCOH is the carbene conformer that shows the greatest changes in the atomic charges and is also the only one that has a transition state.

The local properties of $\rho(\mathbf{r})$ provide information complementary to the atomic properties. The behavior of the local properties of the electron density is well illustrated by the electron density itself, evaluated at the bond critical points, and also by the Laplacian of the electron density ($\nabla^2\rho(\mathbf{r})$) in several regions of a molecule. Figure 5 displays the values of $\rho(\mathbf{r})$ at each of the three bond critical points for each conformer. As expected, the electron density at the O−H bond critical point decreases to approximately zero at long distances. This behavior is consistent with the breaking of the O−H bond. It is also interesting that, whereas at the H−C bond critical point $\rho(\mathbf{r})$ remains almost unchanged, the value at the C−O bond critical point increases with the formation of the radicals due to an increase in the double-bond character. This is in contrast to formaldehyde, whose electron density at the C−O bond critical point changes by only 0.013 atomic unit.

The Laplacian of the electron density also provides important information about the changes in the electronic structure of the conformers of HCOH during dissociation. These changes can be followed by the local charge concentrations indicated by the existence and location of local minima exhibited by this property. Figure 6 shows contours of $\nabla^2\rho(\mathbf{r})$ for some selected molecular geometries in each case. At short O−H bond distances there are regions of negative values of the $\nabla^2\rho(\mathbf{r})$ that correspond to two electron pairs, one each for the carbon and oxygen atoms. The occurrence of only one critical point corresponding to a minimum in the Laplacian of the electron density in the nonbonded region of the oxygen atom deserves some attention. In methanol, for example, two critical points are found above and below the C−O−H plane.[27,46] However, in hydroxycarbene one of these oxygen lone pairs donates electron density into the virtual p-orbital of the carbon atom to form a partial π bond, resulting in the observation of only one oxygen lone pair in the

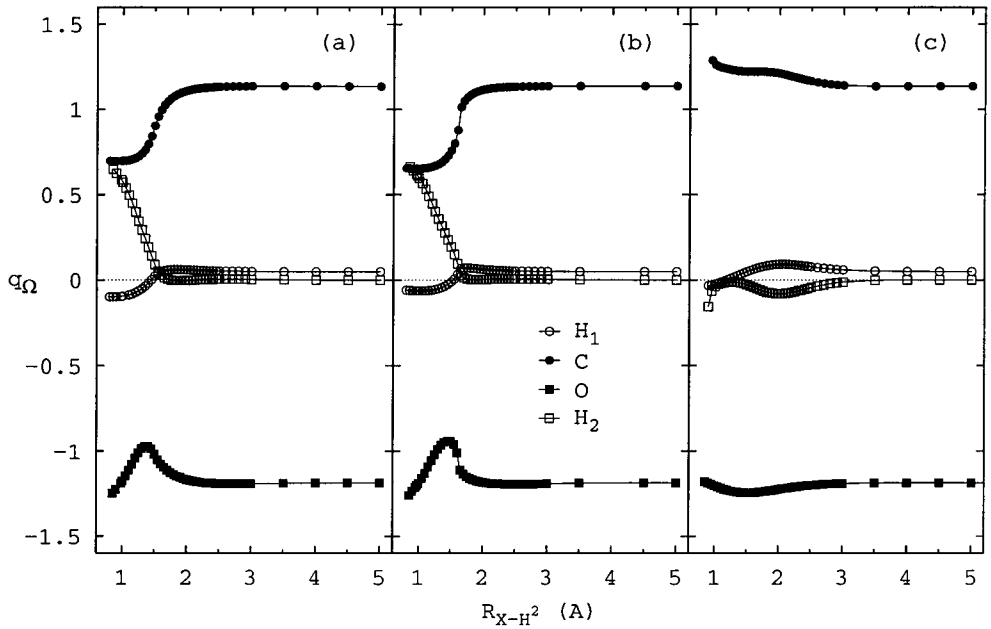

Figure 4. MRCI(8,8) atomic charges for (a) *cis*-HCOH, (b) *trans*-HCOH, and (c) H_2CO.

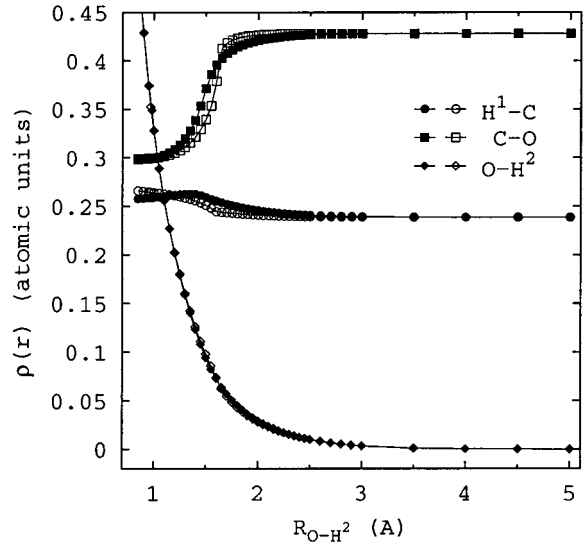

Figure 5. Electron density for the three bond critical points in *cis*- and *trans*-HCOH versus the reaction coordinate using the MRCI(8,8) wave functions.

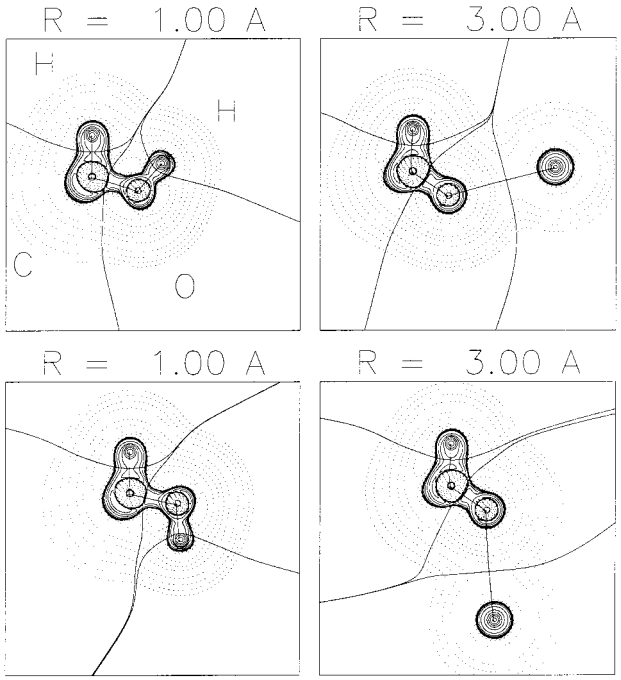

Figure 6. Contours of the Laplacian of the electron density for some selected molecular geometries from the MRCI(8,8) wave functions. Dashed and solid lines correspond to positive and negative values of $\nabla^2\rho(\mathbf{r})$, respectively.

H−C−O−H plane. Figure 7 shows how the value of $\nabla^2\rho(\mathbf{r})$ at the carbon lone pair critical point becomes less negative during dissociation. The most important changes take place for O−H separations in the vicinity of the avoided crossing of the two lowest singlet electronic states. This trend can be attributed to the transition from the carbene to the formyl radical and supports the contention that it is the carbon atom that donates an electron to hydrogen. It was also found that the oxygen lone pair that develops with the homolysis of the O−H bond begins to appear immediately following the avoided crossing for *trans*-HCOH. However, the lone pair does not begin to develop for the cis conformer until the H−O bond length has reached ∼2.7 Å. This shows that the cis conformer undergoes a smoother change to radicals compared to *trans*-HCOH.

To this point, the examination of the electronic properties has indicated that the avoided crossing involves a substantial reordering of the electronic structure of both HCOH conformers, suggesting that a transition state might be expected. However, there has been no indication of why only one conformer has such a transition state. Careful analysis of the dipole moment in terms of its charge transfer and polarization contributions seems to provide an explanation for the differences observed in the potential energy curves of these conformers. Examination of Figures 8 and 9 indicates that the main differences between the dipole moments of *cis*- and *trans*-HCOH occur on the carbene side of the potential energy curve. At these short distances, $\boldsymbol{\mu}_p$ and $\boldsymbol{\mu}_{ct}$ are nearly parallel for *trans*-HCOH and almost cancel each other. As the magnitude of the polarization contribution $|\boldsymbol{\mu}_p|$ is slightly greater than that of the charge transfer $|\boldsymbol{\mu}_{ct}|$, the former determines the direction of $\boldsymbol{\mu}$. This greater polarization of the charge distribution can be associated with the lone pairs on the carbon and oxygen atoms. In the case of *cis*-HCOH, the ratio $|\boldsymbol{\mu}_p|/|\boldsymbol{\mu}_{ct}|$ is similar to the one for

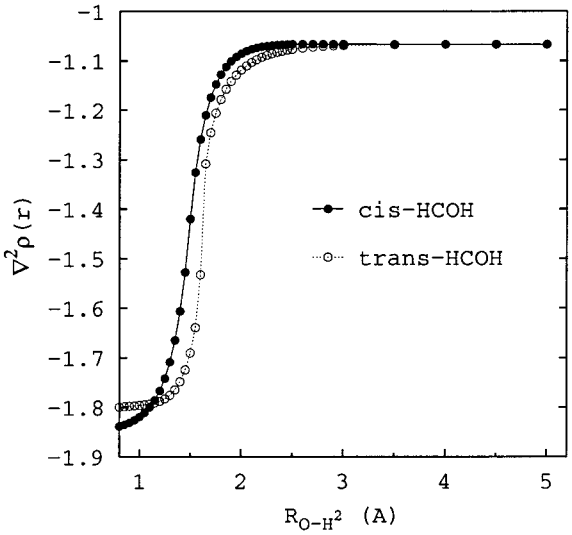

Figure 7. Laplacian of the electron density at the critical point corresponding to the carbon lone pair as it becomes a radical center for both HCOH isomers, calculated using the MRCI(8,8) wave functions.

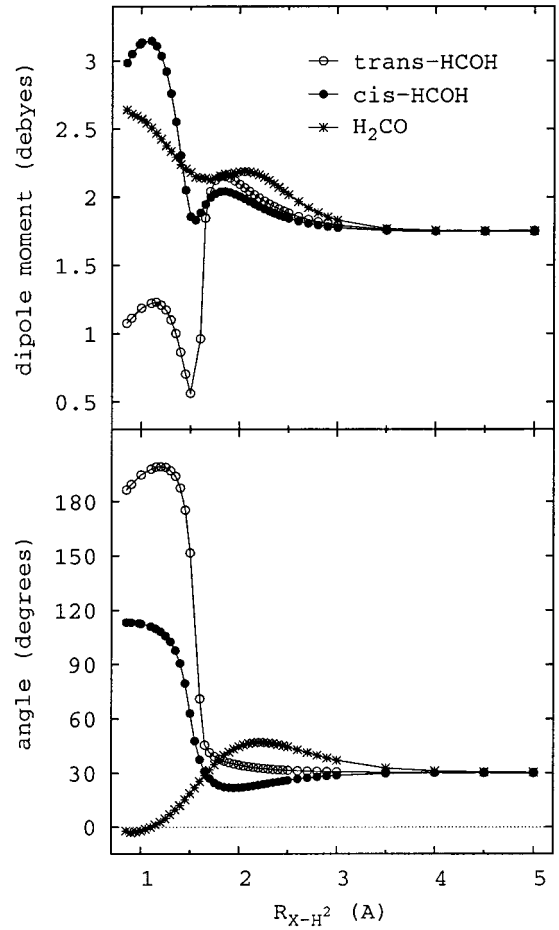

Figure 8. Magnitude and angle, relative to the C−O bond, of the dipole moment for *cis*-HCOH, *trans*-HCOH, and H_2CO. A positive angle corresponds to a clockwise rotation about the *z*-axis.

the other conformer. However, in this case the vectors are oriented in a different manner, with a less effective cancellation between contributions, resulting in a greater dipole moment for *cis*-HCOH whose direction clearly differs from that of the trans conformer. This is a consequence of the relative positions of the lone pairs for each conformer. On the other hand, after the avoided crossing of states, $\boldsymbol{\mu}_{ct}$ and $\boldsymbol{\mu}_{p}$ are oriented in an antiparallel manner in both cases, with a dominant contribution of the charge transfer. This greater contribution of $\boldsymbol{\mu}_{ct}$ to $\boldsymbol{\mu}$ is in part due to the increase of the charge transfer from carbon to oxygen, as indicated by the atomic charges in Figure 4. The dominance of the charge-transfer component of $\boldsymbol{\mu}$ in the formyl radical is similar to what has been previously reported for carbonyl compounds.[47]

It is apparent from Figures 8 and 9 that the trans conformer has to undergo greater changes in its dipole moment during dissociation. After the avoided crossing of states, the radicals for both isomers have very similar dipole moments and proceed to the same limit. Before the avoided crossing of states the magnitude of the dipole moment decreases for both conformers. In the case of *trans*-HCOH, $|\boldsymbol{\mu}|$ is greater than that of the radical and initially moves away from the final value of the formyl radical. On the other hand, *cis*-HCOH starts with a $|\boldsymbol{\mu}|$ smaller than that of the radical and approaches the final value earlier during the homolysis. Hence, the electronic structures of the crossing electronic states do not properly match for *trans*-HCOH, and the isomer is forced to undergo greater adjustments in its charge distribution during the avoided crossing. This is in contrast to the dipole moment of formaldehyde, which decreases smoothly to the common dissociation limit of all three isomers. The energetic cost of these adjustments in the electronic structure, as well as the greater buildup in charge concentrations demonstrated above, results in the occurrence of a transition state for *trans*-HCOH.

4.3. Geometries. Figures 10 and 11 show the evolution of the internal coordinates as a function of the reaction coordinate at the CAS(8,8) level. Similar behavior was found for the 10,10 active space. As can be seen, the most important changes take place in the vicinity of the avoided crossing. In the case of *trans*-HCOH these changes occur later and in a narrower interval around the transition state. This is in keeping with a delayed avoided crossing for the trans with respect to the cis conformer. The decreasing C−O bond distance presented in Figure 10 indicates increasing double bond character and parallels the increasing electron density at the C−O bond critical point already discussed (Figure 5). It is interesting to note that the H−C bond distances and the H−C−O bond angles reflect the behavior observed for the dipole moments (Figure 8), in the sense that the geometry of the *cis*-HCOH carbene approaches that of the radical in the region of the avoided crossing. On the other hand the trans conformer does not display this convergent behavior. This is a consequence of the differences in the electronic structure of the two states involved in the avoided crossing.

5. Conclusion

Homolytic fragmentations of simple molecules generally proceed without a transition state. The homolysis of oxy- and dioxycarbenes seems to be an exception to this statement. The comparisons made for the changes in the molecular geometry of the conformers of HCOH during dissociation, along with the discussion of the behavior of the electronic structures, provide an explanation as to why there is a transition state for the trans and not for the cis conformer. It appears that the necessary changes in electron configuration for the conversion of the carbenes to radicals involve a substantial reorganization of the electron density, as described, for example, by its Laplacian and by the analysis of the atomic charges. The analysis of the dipole moment summarizes the changes taking place in the electron density during the homolysis. In the case of *trans*-HCOH the dipole moments are very different just before and

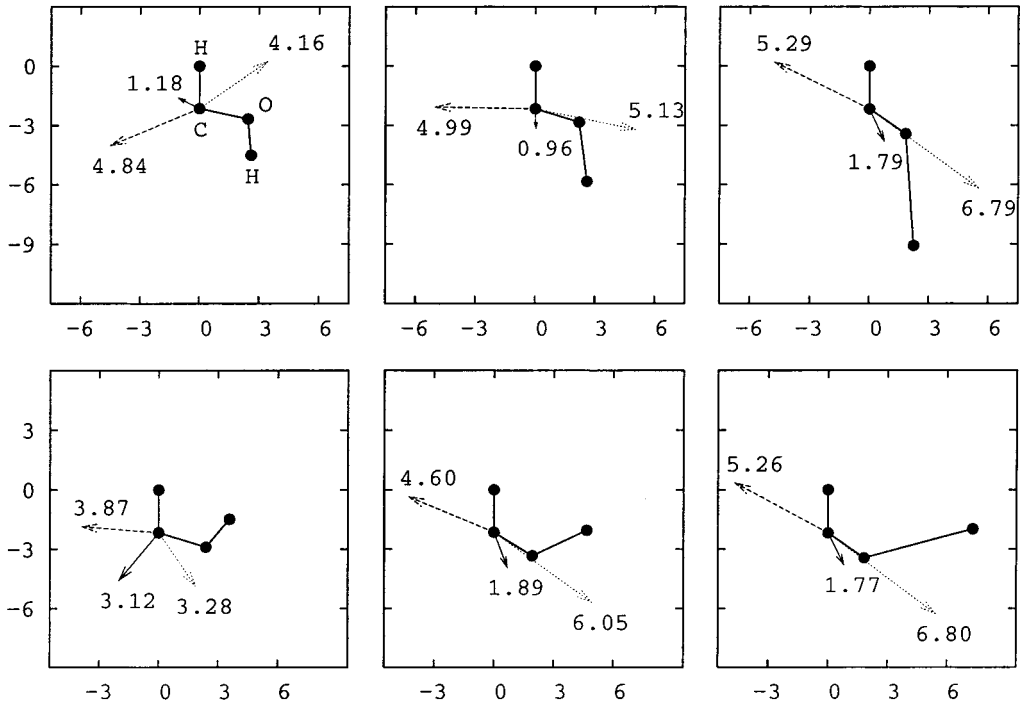

Figure 9. Dipole moment (μ), its corresponding charge transfer (μ_{ct}), and polarization (μ_p) components for some selected geometries of *trans*-HCOH in the top row and *cis*-HCOH in the bottom row. Arrows point in the direction of the negative end of the dipole. Magnitudes are shown in atomic units.

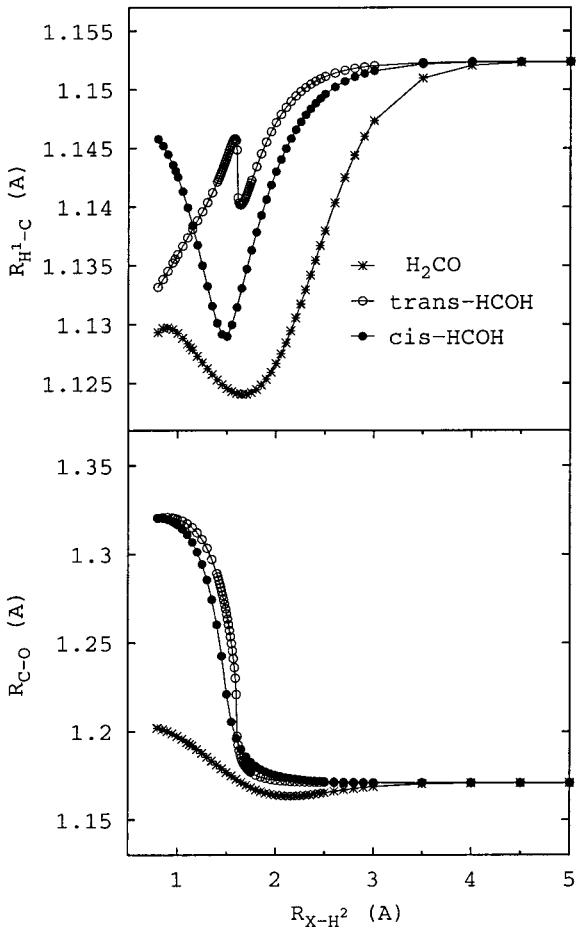

Figure 10. H−C and C−O bond distances versus the reaction coordinate for *cis*-HCOH, *trans*-HCOH, and H_2CO at the CAS(8,8) level of theory.

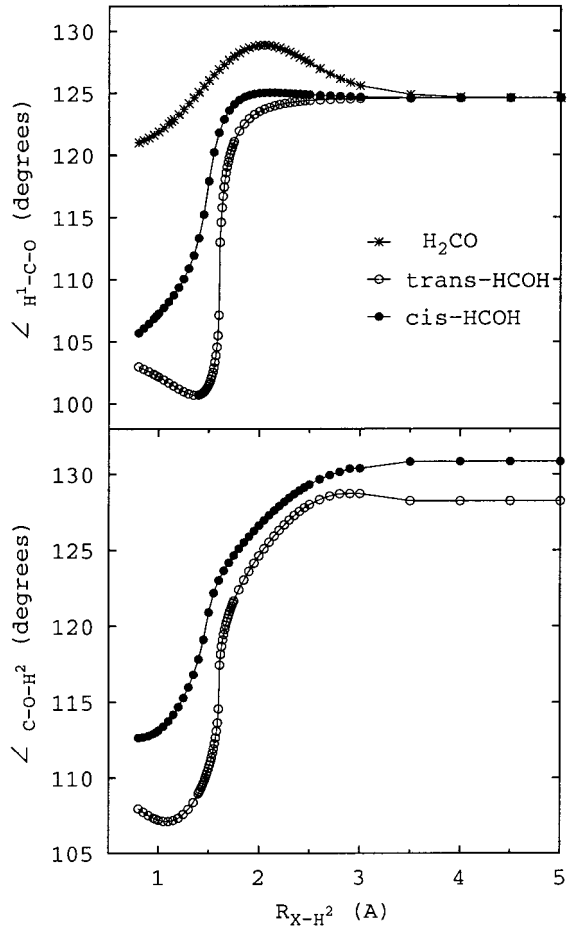

Figure 11. Relevant bond angles in the dissociation of *cis*- and *trans*-HCOH and of H_2CO versus the reaction coordinate at the CAS(8,8) level of theory.

after the avoided crossing of states, resulting in electronic and geometric adjustments which raise the energy of the homolysis and lead to a transition state. The transition state observed here for *trans*-HCOH, and probably for w-dihydroxycarbene, studied

by Borden,[22] appears to be caused by a mismatch in the electronic structures of the states involved, rather than by an inadequacy of the level of calculation used.

Some mention should be made of the possible generality of this reaction. It is clear that similar homolyses have been observed a number of times, usually under what would be considered harsh conditions. Moreover, for substituted oxycarbenes it seems reasonable to anticipate much lower dissociation energies than those calculated here for HCOH. For example, as a consequence of the increased stability of an allyl radical versus a hydrogen atom, the homolysis of allyloxycarbene to formyl and allyl radicals should involve a lower dissociation energy than for HCOH. As a result, homolysis of oxy- and dioxycarbenes from the singlet ground state could be a facile pathway for a wide range of oxycarbenes.

Acknowledgment. The authors are grateful to the Natural Sciences and Engineering Research Council of Canada for funding. J.H.-T. thanks CONACYT-México for financial support. We also thank Dr. J. R. Kramer and P. V. Collins for supplying computing support and facilities, funded by NSERC, and Dr. R. F. W. Bader and Dr. G. L. Heard for helpful discussions.

References and Notes

(1) Heydt, H.; Regitz, M. Carbene(oide). In *Methoden der Organischen Chemie (Houben-Weyl)*; Regitz, M., Ed.; Georg Thieme Verlag: Stuttgart, Germany, 1989; Vol. E19b, Parts 1 and 2, pp 1−1901.

(2) Moss, R. A. In *Advances in Carbene Chemistry*; Brinker, U. H., Ed.; JAI Press: London, England, 1994; Vol. 2, pp 59−88.

(3) Moss, R. A. *Pure Appl. Chem.* **1995**, *67*, 741−747.

(4) Yates, P.; Loutfy, R. O. *Acc. Chem. Res.* **1975**, *8*, 209−216.

(5) Hemminger, J. C.; Rusbult, C. F.; Lee, E. K. C. *J. Am. Chem. Soc.* **1971**, *93*, 1867−1871.

(6) Lee-Ruff, E.; Hopkinson, A. C.; Kazarians-Moghaddam, H. *Tetrahedron Lett.* **1983**, *24*, 2067−2070.

(7) Foster, A. M.; Agosta, W. C. *J. Am. Chem. Soc.* **1973**, *95*, 608−609.

(8) Smith, A. B., III.; Foster, A. M.; Agosta, W. C. *J. Am. Chem. Soc.* **1972**, *94*, 5100−5101.

(9) Foster, A. M.; Agosta, W. C. *J. Am. Chem. Soc.* **1972**, *94*, 5777−5781.

(10) Ayral-Kaloustian, K.; Agosta, W. C. *J. Org. Chem.* **1982**, *47*, 284−287.

(11) Borden, W. T.; Hoo, L. H. *J. Am. Chem. Soc.* **1978**, *100*, 6274−6276.

(12) McDonald, R. M.; Krueger, R. A. *J. Org. Chem.* **1966**, *31*, 488−494.

(13) Crawford, R. J.; Raap, R. *Proc. Chem. Soc., London* **1963**, 370.

(14) Lemal, D. M.; Gosselink, E. P.; McGregor, S. D. *J. Am. Chem. Soc.* **1966**, *88*, 582−600.

(15) Lemal, D. M.; Lovald, R. A.; Harrington, R. W. *Tetrahedron Lett.* **1965**, 2779−2785.

(16) Wong, T.; Warkentin, J.; Terlouw, J. K. *Int. J. Mass Spectrom. Ion Processes* **1992**, *115*, 33−52.

(17) Suh, D.; Pole, D. L.; Warkentin, J.; Terlouw, J. K. *Can. J. Chem.* **1996**, *74*, 544−558.

(18) Hoffmann, R. W.; Hirsch, R.; Fleming, R.; Reetz, M. T. *Chem. Ber.* **1972**, *105*, 3532−3541.

(19) Venneri, P. C.; Warkentin, J. *J. Am. Chem. Soc.* **1998**, *120*, 11182−11183.

(20) Altmann, J. A.; Csizmadia, I. G.; Yates, K.; Yates, P. *J. Chem. Phys.* **1977**, *66*, 298−302.

(21) Altmann, J. A.; Csizmadia, I. G.; Robb, M. A.; Yates, K.; Yates, P. *J. Am. Chem. Soc.* **1978**, *100*, 1653−1657.

(22) Feller, D.; Borden, W. T.; Davidson, E. R. *J. Comput. Chem.* **1980**, *1*, 158−166.

(23) Goddard, J. D.; Schaefer, H. F., III. *J. Chem. Phys.* **1979**, *70*, 5117−5134.

(24) Kakumoto, T.; Saito, K.; Imamura, A. *J. Phys. Chem.* **1987**, *91*, 2366−2371.

(25) Bader, R. F. W. *Atoms in Molecules. A Quantum Theory*; Clarendon: Oxford, 1990.

(26) Bader, R. F. W.; Beddall, P. M.; Cade, P. E. *J. Am. Chem. Soc.* **1971**, *93*, 3095−3107.

(27) Bader, R. F. W.; Essén, H. *J. Chem. Phys.* **1984**, *80*, 1943−1960.

(28) Gillespie, R. J.; Robinson, E. A. *Angew. Chem., Int. Ed. Engl.* **1996**, *35*, 495−514.

(29) Schmidt, M. W.; Baldridge, K. K.; Boatz, J. A.; Elbert, S. T.; Gordon, M. S.; Jensen, J. H.; Koseki, S.; Matsunaga, N.; Nguyen, K. A.; Su, S. J.; Windus, T. L.; Dupuis, M.; Montgomery, J. A. *J. Comput. Chem.* **1993**, *14*, 1347−1363.

(30) Dunning, T. H., Jr. *J. Chem. Phys.* **1989**, *90*, 1007−1023.

(31) Biegler-König, F. W.; Bader, R. F. W.; Tang, T.-H. *J. Comput. Chem.* **1982**, *3*, 317−328.

(32) Frisch, M. J.; Trucks, G. W.; Schlegel, H. B.; Gill, P. M. W.; Johnson, B. G.; Robb, M. A.; Cheeseman, J. R.; Keith, T.; Petersson, G. A.; Montgomery, J. A.; Raghavachari, K.; Al-Laham, M. A.; Zakrzewski, V. G.; Ortiz, J. V.; Foresman, J. B.; Cioslowski, J.; Stefanov, B. B.; Nanayakkara, A.; Challacombe, M.; Peng, D. Y.; Ayala, P. Y.; Chen, W.; Wong, M. W.; Andres, J. L.; Replogle, E. S.; Gomperts, R.; Martin, R. L.; Fox, D. J.; Binkley, J. S.; Defrees, D. J.; Baker, J.; Stewart, J. P.; Head-Gordon, M.; Gonzalez, C.; Pople, J. A. *Gaussian 94, Revision E.2*; Gaussian, Inc.: Pittsburgh, PA, 1995.

(33) Deng, L.; Ziegler, T.; Fan, L. *J. Chem. Phys.* **1993**, *99*, 3823−3835.

(34) Kamiya, K.; Morokuma, K. *J. Chem. Phys.* **1991**, *94*, 7287−7298.

(35) Räsänen, M.; Raaska, T.; Kunttu, H.; Murto, J. *J. Mol. Struct. (THEOCHEM)* **1990**, *208*, 79−90.

(36) Goddard, J. D.; Yamaguchi, Y.; Schaefer, H. F., III. *J. Chem. Phys.* **1981**, *75*, 3459−3465.

(37) Frisch, M. J.; Krishnan, R.; Pople, J. A. *J. Phys. Chem.* **1981**, *85*, 1467−1468.

(38) Harding, L. B.; Schlegel, H. B.; Krishnan, R.; Pople, J. A. *J. Phys. Chem.* **1980**, *84*, 3394−3401.

(39) Benson, S. W. *Thermochemical Kinetics*, 2nd ed.; Wiley: New York, 1976.

(40) Pau, C. F.; Hehre, W. J. *J. Phys. Chem.* **1982**, *86*, 1252−1253.

(41) Lucchese, R. R.; Schaefer, H. F., III. *J. Am. Chem. Soc.* **1978**, *100*, 298−299.

(42) Sheridan, R. S.; Moss, R. A.; Wilk, B. W.; Shen, S.; Wostowski, M.; Kesselmayer, M. A.; Subramanian, R.; Kmiecik-Lawrynowicz, G.; Krogh-Jespersen, K. *J. Am. Chem. Soc.* **1988**, *110*, 7563−7564.

(43) Moss, R. A.; Wostowski, M.; Shen, S.; Krogh-Jespersen, K.; Matro, A. *J. Am. Chem. Soc.* **1988**, *110*, 4443−4444.

(44) Bruna, P. J.; Buenker, R. J.; Peyerimhoff, S. D. *J. Mol. Struct.* **1976**, *32*, 217−233.

(45) Feller, D.; Davidson, E. R. *J. Chem. Phys.* **1984**, *80*, 1006−1017.

(46) Esseffar, M.; El Mouhtadi, M.; López, V.; Yáñez, M. *J. Mol. Struct. (THEOCHEM)* **1992**, *255*, 393−408.

(47) Slee, T.; Larouche, A.; Bader, R. F. W. *J. Phys. Chem.* **1988**, *92*, 6219−6227.